# Image Segmentation in Complex Basis of Type-2 Membership Functions Subspace

Lyudmila Akhmetshina[1,†], Artyom Yegorov[1,*,†], Artem Fomin[1,†]

[1] *Oles Honchar Dnipro National University, Nauki Avenue, house 72, Dnipro, 49010, Ukraine*

## Abstract

A new method for grayscale image segmentation based on the type-2 fuzzy clustering method (T2FCM) is presented. This method enhances segmentation sensitivity, reliability, and noise immunity. The proposed algorithm is based on the orthogonalization of fuzzy membership functions using singular value decomposition, the formation of a complex space of orthogonal eigenvalues, and the synthesis of a composite resulting image based on these components. Experimental results are provided for images of various physical nature.

## Keywords

Image Segmentation, Type-2 Fuzzy Clustering, complex singular subspaces1

## 1. Introduction

Digital images, which are the output of standard research methods in various fields such as materials science, medicine, and defectoscopy, often suffer from insufficient quality for reliable analysis. To make these images more suitable for specific applications, improve their interpretability by humans, or enable their use in automated systems, appropriate transformations are required [1].

Medical images (such as tomograms, fluorograms, and mammograms), which serve as essential diagnostic tools for numerous diseases, are characterized by low intensity, uneven background, high noise levels, low contrast, and poorly defined structural boundaries. These images are particularly challenging to make their analysis and the selection of an effective processing method. Typically, the shape, position (and sometimes even the presence), and characteristics of the object of interest (pathology or anomaly) in the analyzed image are unknown a priori. As a result, distinguishing structural (anatomical) and measurement noise from the useful signal is particularly difficult, especially given that the statistical and spectral properties of these noise components are also usually unknown.

In this context, segmentation methods for objects of interest in images hold significant practical value, particularly when there is virtually no prior information about the data distribution. These methods rely on assessing the proximity of object parameters in a multidimensional space, guided only by heuristic assumptions about the nature and features of the studied dataset.

By objects of interest or anomalies, we refer to observations that deviate from the rest of the data, have characteristics different from those of neighboring image regions, have unknown location and shape a priori, and whose identification is the primary goal of analysis. The complexity of detecting such anomalies lies in the fact that, on the one hand, they often represent small regions that can be mistaken for noise or image artifacts. On the other hand, their parameters may only slightly differ from the general background or be obscured by other objects.

Modern approaches to solving this problem widely employ fuzzy logic, particularly, fuzzy clustering methods, which enable more precise object segmentation, noise differentiation, and detail restoration while ensuring greater robustness to distortions and defects arising during image formation [2–5].

*ICST-2025: Information Control Systems & Technologies, September 24-26, 2025, Odesa, Ukraine*

* Corresponding author.

† These authors contributed equally.

akhmlu1@gmail.com (L. Akhmetshina); for___students@ukr.net (A. Yegorov); fominartempost@gmail.com (A. Fomin)

0000-0002-5802-0907 (L. Akhmetshina); 0000-0002-7558-785X (A. Yegorov); 0009-0006-0684-0811 (A. Fomin)

Currently, no universal methods guarantee reliable segmentation results for images with diverse physical properties. Therefore, the development of new algorithms tailored to specific tasks remains an ongoing research challenge [6–8].

## 2. Review of literature

The problem of image processing is closely related to the task of information extraction. Digital image processing algorithms are highly specific, and their performance depends significantly on both the characteristics of the input data (such as noise, blurring, background intensity variations, brightness, and contrast) and the objectives of the analysis.

Since 1965, type-1 fuzzy sets (FST1) have been successfully applied in various image processing applications, allowing for the consideration of uncertainty and ambiguity, which are always present in the original data [9].

A distinctive feature of fuzzy methods is that input data are transformed into a fuzzy space, where further processing is performed. For an image $I(x,y)$, where $x, y$ are the pixel coordinates, a membership function is defined, which takes numerical values in the range [0,1] and represents the degree to which a particular property is exhibited (such as grayscale level, histograms, and other features) [10].

Studies [11–14] demonstrate the effectiveness of FST1 in segmenting images with various physical properties. For instance, in medical imaging, where segmentation is used to differentiate tissues (such as bone, muscle, and fat), FST1-based fuzzy clustering allows for more precise object extraction, noise differentiation, and detail restoration, providing greater robustness against distortions and artifacts introduced during image formation.

However, a key limitation of FST1 is that it represents uncertainty in the input data as a single crisp value, which restricts its ability to describe other types of uncertainty and ambiguity. These include variability associated with the estimation of membership functions, processing algorithms, measurement errors, or image acquisition systems [15].

To address these limitations, type-2 fuzzy sets (FST2) have been introduced, offering improvements over traditional FST1-based segmentation methods. Research in [16–18] has demonstrated that FST2 enables more precise object segmentation, while [19] shows its effectiveness in restoring images corrupted by noise. Additionally, [20] highlights its improved ability to handle uncertainties that arise during image processing.

## 3. Problem statement

The objective of this paper is to present a new grayscale image segmentation method based on type-2 fuzzy clustering (T2FCM). The proposed method enhances segmentation sensitivity, reliability, and noise immunity by orthogonalizing fuzzy membership functions using singular value decomposition, constructing a complex space of orthogonal eigenvalues, and synthesizing a composite resulting image based on these components.

## 4. Materials and Methods

For an image $I(x,y)$ of size $[dx \times dy]$, the result of type-1 fuzzy clustering (FCMT1) is a three-dimensional matrix $U$, which contains the membership function values for each pixel $u_{x,y}$ in relation to the properties being analyzed (e.g., brightness, homogeneity, edges, background). The dimensionality of the third coordinate is determined by the predefined number of clusters $c$. Traditionally, defuzzification (the formation of a final result in a crisp space) is performed based on the maximum membership function value. However, this approach is suboptimal because membership functions may exhibit multiple extrema of comparable or even equal amplitude, and no prior information is available regarding the significance of a particular cluster. This can result in the loss of valuable information.

Figure 1 a presents an image of the microstructure of a ternary eutectic alloy in multicomponent systems, which is analyzed in quantitative metallography to determine its characteristics (such as the volume fraction of various phases, grain size, and specific grain boundary surface area). Figure 1 b shows its histogram. The image is characterized by an uneven background, noise, and low

contrast, while its histogram does not allow for the identification of a brightness range corresponding to the objects of interest. Figures 1 d, 1 e, and 1 f depict three different fuzzy classes obtained by applying FCMT1 with six clusters, enabling the visualization of individual structures of the alloy that are the focus of analysis. In contrast, the defuzzification result based on the maximum membership function (Figure 1 c) lacks meaningful analytical information, producing a noise-like pattern.

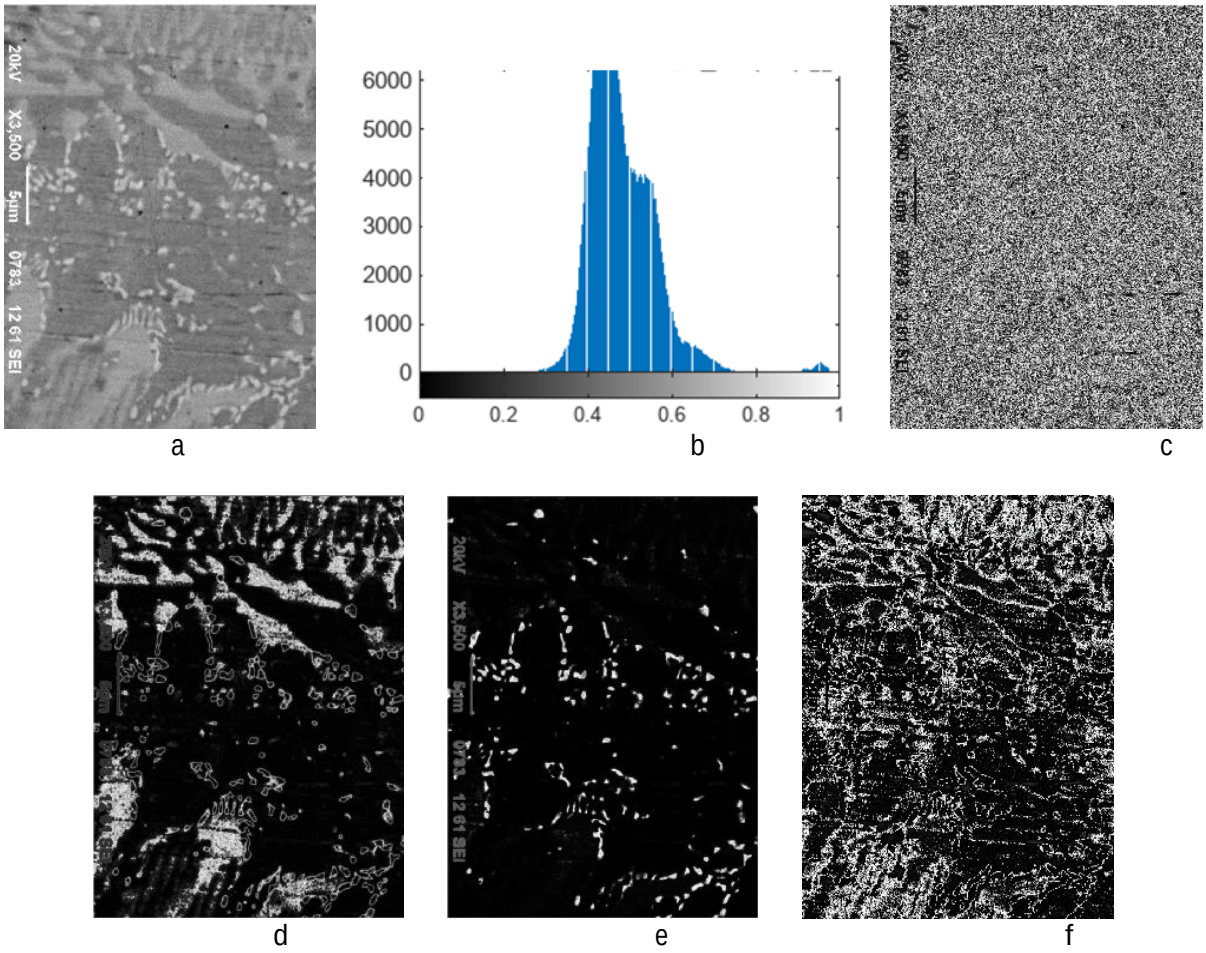


Figure 1: Different visualization approaches for fuzzy clustering results using the FCMT1 method: a – original metallographic image; b – its histogram; c – maximum membership function; d, e, f – visualization of three arbitrary classes.

In type-2 fuzzy sets (FST2), the membership function of each element can itself be represented as a function. If the membership function $u$ of a type-1 fuzzy set (FST1) is defined, the corresponding lower $u_l$ and upper $u_h$ membership functions used to describe FST2 can be determined using the expressions:

$$u_l(i,j) = u(g(i,j))^{\alpha(i,j)}, \quad (1)$$

$$u_h(i,j) = u(g(i,j))^{\frac{1}{\alpha(i,j)}}, \quad (2)$$

where $\alpha \in (1,\infty)$ is the transformation coefficient [20].

FST1 is characterized by its degree of fuzziness, whereas FST2 is defined by its degree of uncertainty (second-order uncertainty – "fuzzy fuzzy sets") [15]. In FST1, the fuzzy representation of the initial parameter is lost after transformation, eliminating all uncertainty (Figure 2 a). In contrast, FST2 introduces a third dimension, represented by the footprint of uncertainty (FOU) (Figure 2 b). Consequently, defuzzification in FST2 involves a more complex two-step process compared to traditional FST1.

Since the membership functions generated by fuzzy clustering are informationally equivalent, image segmentation based on them remains one of the most uncertain and challenging problems. We propose a defuzzification method based on two key ideas: orthogonalization and transformation

into a complex space. This approach allows for analyzing the entire set of membership functions as a unified whole while simultaneously interpreting the result as an anisotropic filtering process in the fuzzy space [21, 22].

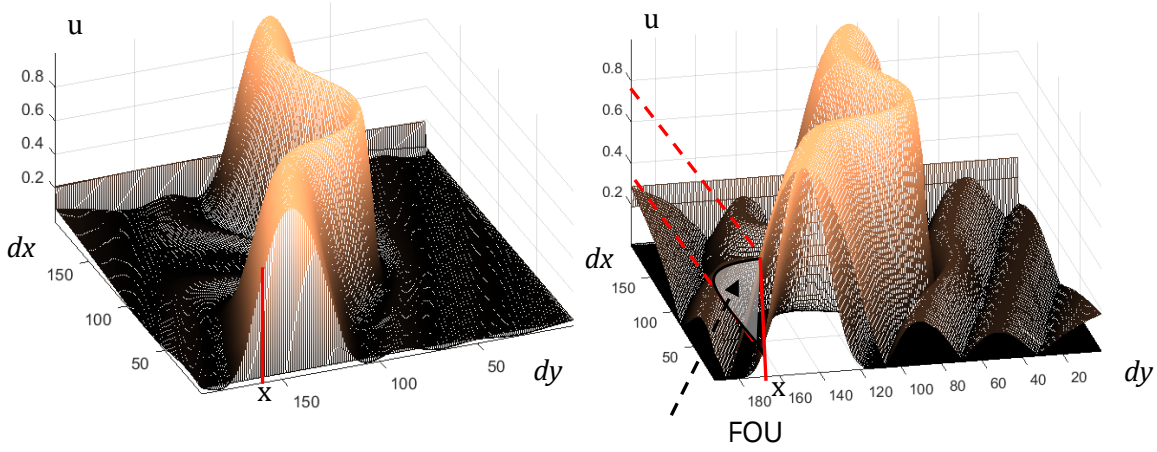


Figure 2: Defuzzification of the membership function: a – FST1 ⟶ crisp value; b – FST2 ⟶ FST1.

Orthogonalization ensures the formation of a non-equivalent eigen-space of membership functions, referred to as orthonormal membership functions (OMF) $G_i(x,y), i=1,...,c$. The first "composite" OMF carries the most significant information regarding $U$, while the second contains the most significant remaining information, and so on. The resulting representation expresses membership functions as a spectrum in the eigen-basis, meaning that preserving only a few principal spectral components is sufficient to retain the essential information from the original data. A crucial aspect of this approach is the ability to assess the informativeness of each component: each $G_i(x,y)$ contains $D_i\%$ of the total information embedded in the original data, as determined by the magnitude of its eigenvalues [23].

The orthonormal property is then used to transition into the complex space of OMF and to synthesize additional informative characteristics based on the expressions:

$$\Phi_i(x,y) = \left[G_k(x,y) + jG_l(x,y)\right],\ k=1,...,c; l=1,...,c, \tag{3}$$

$$\beta_i = \left|\Phi_i\right|, \tag{4}$$

$$\phi_i = angle(\Phi_i), \tag{5}$$

where $k$, $l$ are the corresponding eigenvalues. This provides greater flexibility in analyzing results compared to working within the domain of real brightness values. When operating in the complex domain, various options for mapping the final results (both linear and nonlinear) become possible [24].

The proposed algorithm includes the following steps:

1. Making window transformation (window size 3x3) brightness values of the original greyscale image $I$ by using a window transformation and forming in that way a 9-dimensional ensemble including the brightness of neighbouring pixels to take into account for spatial characteristics. This constitutes the first stage of expanding the input data space.
2. Performing an orthogonal transformation (SVD) of the expanded original data with subsequent automatic selection of the most significant components [25] based on calculating the coefficient vector $C$ as follows:

$$C_i = \frac{\left|\sum_{j=1}^{1+c}(V_s)_{i,j}\right| + \left|\sum_{j=1}^{1+c}(V_s)_{j,i}\right|}{2}, i \in [1,1+c], \tag{6}$$

where $V_s$ contains the right singular vectors for the SVD. Vector $C$ is sorted in descending order. A difference vector $dC$ is also created containing the differences for each neighbouring pair in the sorted vector $C$. The value $dC_a$ is calculated by the next formula:

$$dC_a = \frac{\sum_{j=1}^{c} \frac{dC_j}{c} + \frac{dC_{\min} + dC_{\max}}{2}}{2}, \tag{7}$$

where $dC_{\min}$ and $dC_{\max}$ are the minimum and maximum elements of vector $dC$, correspondingly. This threshold value $dC_a$ is used to determine the number of the most significant elements of the left singular vector matrix. The selected indices correspond to the original indices in vector $C$ prior to sorting $I^{svd}$.

3. Scaling each component of matrix $I^{svd}$ to the range $[0,1]$.

4. The second stage of data space expansion involves generating matrices $\mathrm{A}$ and $\Sigma$ for each pair of components of the matrix $I^{svd}$ with indices $k$, $l$ according to the following formulas:

$$\mathrm{A} = \left| I_k^{svd} + jI_l^{svd} \right|, \tag{8}$$

$$\Sigma = \left( angle\left( I_k^{svd} + jI_l^{svd} \right) + angle\left( I_l^{svd} + jI_k^{svd} \right) \right) / 2. \tag{9}$$

These matrices are then scaled to the range $[0,1]$, and a new component of the three-dimensional matrix $I^c$ (the total number of components equals the number of all possible pairs of components from $I^{svd}$) is computed using the following formulas:

$$I_j^c = \mathrm{A} \cdot (1 - K_2) + \Sigma \cdot K_2, \tag{10}$$

$$K_2 = K_1 + \bar{\Sigma}^{1-\bar{\mathrm{A}}} - \bar{\mathrm{A}}^{1-\bar{\Sigma}}, \tag{11}$$

$$K_1 = K_0 + \frac{0.5 - \bar{I}}{1 + \frac{\bar{I} + K_0}{2}}, \tag{12}$$

where $\bar{I}$, $\bar{\mathrm{A}}$ and $\bar{\Sigma}$ are the average values of matrices $I$, $\mathrm{A}$ and $\Sigma$, respectively, and $K_0$ is a constant parameter (in experiments values in the range $[0.4,0.6]$ were used). It should be noted that both the value of $K_0$ and the structure of equation (12) were chosen experimentally and significantly affect segmentation sensitivity. Using $K_1$ instead of $K_0$ in equation (11) allows for the consideration of specific characteristics of the processed image.

5. Scaling all components of matrix $I^c$ to the range $[0,1]$, followed by orthogonal transformation SVD and selecting the most significant components according to the algorithm described in Section 2.

6. Merging matrices $I^{svd}$ and the most significant components of $I^c$ into a single matrix $I^{svd-c}$ and forming in that way a multidimensional input matrix for fuzzy data clustering.

7. Performing fuzzy clustering of the scaled matrix $I^{svd-c}$. We used T2FCM method [16] with dynamic compression of the fuzzy membership function [3], which involves initially setting a larger number of fuzzy clusters, which dynamically decreases during training by merging close clusters. The closeness of fuzzy cluster centers is determined by usage of weighted Euclidean distance, which is calculated (for the distance between the centers of the k-th and l-th clusters) by the next formula:

$$d_{k,l}^0 = \sqrt{\sum_{j=1}^{q} \left( S_{u_k} \cdot v_{k,j}^t - S_{u_l} \cdot v_{l,j}^t \right)^2}, \tag{13}$$

where values $S_{u_k}$ and $S_{u_l}$ are calculated as:

$$S_{u_j} = \frac{\overline{u_j}}{u_{\min}}, (\forall j \in \{1,\ldots,c\}), \tag{14}$$

where $\overline{u_j}$ is the average membership function value for the j-th fuzzy cluster, and $\overline{u_{\min}}$ is the minimum value of the vector $\bar{u}$ of average membership values for each cluster.

During each training iteration $t$, the MFT2 matrix $a^t$ is calculated as the difference between the "upper" $u_h^t$ and "lower" $u_l^t$ membership functions by the next formulas:

$$\left(u_{h_1}^t\right)_{i,k} = \left(\left(u^t\right)_{i,k}\right)^{1-\left(\left(u^t\right)_{i,k}\right)^{1+\left(\left(u^t\right)_{i,k}\right)^{1-\left(u^t\right)_{i,k}+\left(\overline{u^t}\right)_k^1-0.5}}}, \quad (15)$$

$$\left(u_{l_1}^t\right)_{i,k} = \left(\left(u^t\right)_{i,k}\right)^{1+\left(\left(u^t\right)_{i,k}\right)^{1-\left(\left(u^t\right)_{i,k}\right)^{1-\left(u^t\right)_{i,k}-\left(\overline{u^t}\right)_k^1+0.5}}}, \quad (16)$$

$$\left(u_{h_2}^t\right)_{i,k} = \left(\left(u^t\right)_{i,k}\right)^{K+0.75+\left(\overline{u^t}\right)_k^1/2}, \quad (17)$$

$$\left(u_{l_2}^t\right)_{i,k} = \left(\left(u^t\right)_{i,k}\right)^{K+1.25+\left(\overline{u^t}\right)_k^1/2}, \quad (18)$$

$$\left(\overline{u^t}\right)_k^1 = \left(\left(\overline{u^t}\right)_k\right)^{1-\max\left(\left(\overline{u^t}\right)_k,1-\left(\overline{u^t}\right)_k\right)}, \quad (19)$$

$$\left(u_h^t\right)_{i,k} = \left(\left(u_{h_1}^t\right)_{i,k} + \left(u_{h_2}^t\right)_{i,k}\right)/2, \quad (20)$$

$$\left(u_l^t\right)_{i,k} = \left(\left(u_{l_1}^t\right)_{i,k} + \left(u_{l_2}^t\right)_{i,k}\right)/2, \quad (21)$$

where $\overline{u^t}_k$ is the average membership for the k-th cluster, and $i \in [1, N]$, $K$ is the coefficient, values of which are recommended to be chosen within the range $[0,0.2]$. This coefficient has a significantly impact the transformation results. The final membership function matrix $a^t$ is interpreted as a multidimensional image.

8. Transforming the matrix $I^{svd-c}$ as follows:

$$I_{i,j}^{tr} = \left(I_h^{svd-c}\right)_{i,j} - \left(I_l^{svd-c}\right)_{i,j}, \quad (22)$$

where $I_h^{svd-c}$ and $I_l^{svd-c}$ are calculated as per formulas (15) and (16), correspondingly, forming matrix $I^{tr}$.

9. Obtaining matrix $I^u$ as the columns union of matrices $I^{tr}$ and $a^t$.

10. Applying the transformation described in step 7 to matrix $I^u$ to compute matrix $a^t$ (formulas (15) – (21)), resulting in matrix $I^{T2}$.

11. Applying an orthogonal transformation (SVD) to the matrix $I^{T2}$. After this, the most significant components are selected from the left singular vectors, as described in step 2. A grayscale image $I^s$ is formed using a weighted sum of selected significant components based on the values of the vector $C$, corresponding to the selected significant components of the left singular vectors, scaled so that their sum equals 1.

12. Generating two output images: $I^{out}$ и $I^{out-c}$. The first output is obtained by applying the adaptive histogram equalization method (using a uniform transformation function) to image $I^s$. The second output image, $I^{out-c}$, is generated based on a pair of matrices: $I^s$ and the first component of matrix $I^{svd}$ using formulas (8)–(12), the coefficient $K_2$ is computed as follows:

$$K_2 = K_1 + \bar{\Sigma}^{1-\bar{\Sigma}} - \bar{A}^{1-\bar{A}}, \quad (23)$$

After that, adaptive histogram equalization (using a uniform transformation function) is also applied to $I^{out-c}$.

## 5. Results

The proposed algorithm was applied for the segmentation of grayscale low-contrast images of various physical origins, including computed tomography (CT) scans of the human brain (Figure 3 a), which was used as a test image due to the known location of the objects of interest, and thoracic spine (Figure 4 a), X-ray images of the cervical spine (Figure 5 a), optical microscopy images (Figure 6 a), and microbiological images (Figure 7 a).

These images were obtained using standard research methods across various fields, including medicine, metallography, and microbiology, however, their quality is not enough sometimes for objective analysis.

These images contain significant dark and/or bright regions with objects of interest that are indistinguishable in the original images due to discrepancies in their brightness characteristics and the psychophysical limitations of human vision.

Figures 3 b – 7 b and Figures 3 c – 7 c illustrate the experimental results of applying the algorithm with the following parameters: $m = 2$, $\varepsilon \le 10^{-5}$, initial number of fuzzy clusters $c = 9$ the experiments were conducted on medical images, and therefore, this amount is more than enough), $K = 0.075$, $K_0 = 0.4803$.

It was found that for some images, the best results could be obtained without applying step 10 in the proposed algorithm (using matrix $I^u$ in step 11 instead of $I^{T2}$ ).

Visual assessment of the segmentation results was chosen due to the limitations of automatic metrics, which do not always reliably distinguish objects of interest from excessive detail in the considered image region.

The algorithm proposed in this article was implemented in the MATLAB R2016a environment running on the Microsoft Windows 10 Pro x64 operating system, version 22H2.

Analysis of the results demonstrates that the proposed algorithm significantly enhances segmentation detail and image contrast. For example, Figure 3 a presents a brain CT scan used for diagnosing the presence of a hematoma and its affected region (outlined by a rectangle). Figure 3 b shows a brain CT scan obtained with the use of a radiopaque contrast agent. While such agents may marginally enhance the visibility of the target region by increasing image contrast, their application poses potential health risks. Therefore, it is preferable to improve image quality through advanced image processing techniques rather than relying on invasive substances. The results of applying the standard FCM algorithm with c = 9 and c = 5 (Figure 3 c and Figure 3 d, respectively) to the original image (Figure 3 a) are visualized based on adaptive histogram equalization of the maximum membership function. This approach results in excessive detailing that obscures the region of hematoma spread, which is clearly identified using the proposed method in Figures 3e and 3f. When visualized in the complex space of orthogonal membership functions, the method exhibits greater sensitivity to low-contrast regions of the image compared to Figure 3 e, despite a lower contrast level.

Figures 4 b, 5 b, 6 b, 4 c, 5 c, and 6 c clearly delineate object boundaries and structures. Figures 6 b and 6 c reveal defects and background variations, while Figures 7 b and 7 c enhance the contrast of objects of interest against a non-uniform background and highlight its features. The analysis confirms that transitioning to the complex space effectively reduces noise components, which aligns with the theoretical justification for using complex-valued components for anisotropic filtering in a fuzzy space.

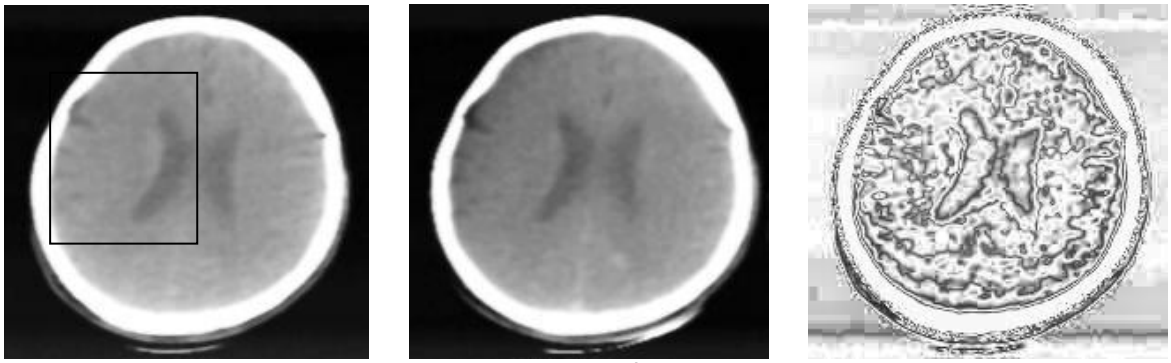

a b c

d e f

Figure 3: Segmentation results of a brain CT scan: (a) original image (204×201); (b) brain CT scan obtained using a radiopaque contrast agent; segmentation using the standard FCM algorithm with different numbers of fuzzy clusters: (c) $c = 9$; (d) $c = 5$; (e) orthogonal membership function space ($I^{out}$); (f) complex orthogonal membership function space ($I^{out-c}$);

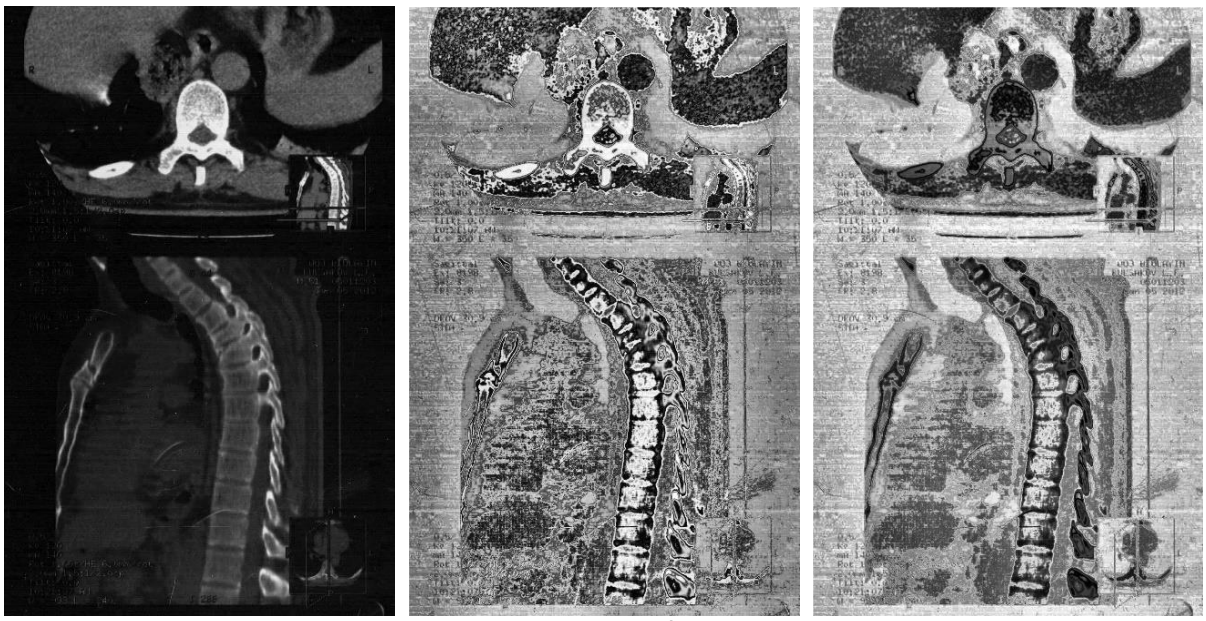

a b c

Figure 4: Segmentation results of a thoracic spine CT scan: (a) original image (1013×1585); (b) orthogonal membership function space ($I^{out}$, without step 10); (c) complex orthogonal membership function space ($I^{out-c}$, without step 10).

a b c

Figure 5: Segmentation results of a cervical spine X-ray: (a) original image (570×744); (b) orthogonal membership function space ($I^{out}$, without step 10); (c) complex orthogonal membership function space ($I^{out-c}$, without step 10).

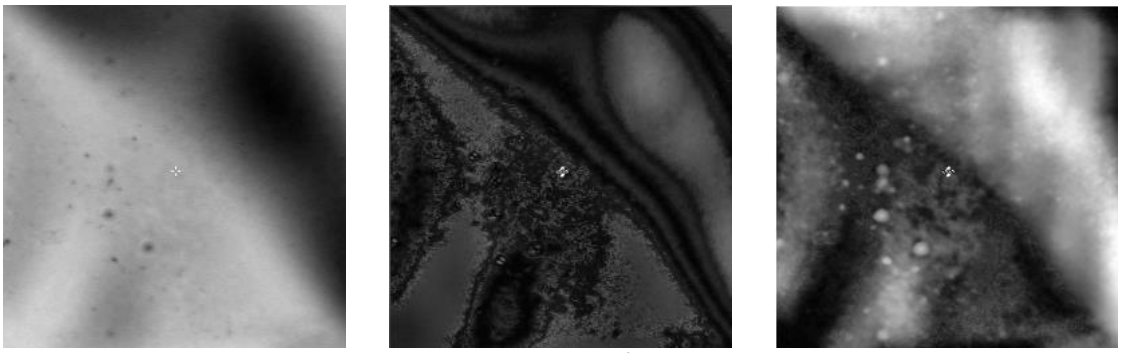

a b c

Figure 6: Segmentation results of an optical membrane image: (a) original image (257×257); (b) orthogonal membership function space ($I^{out}$, without step 10); (c) complex orthogonal membership function space ($I^{out-c}$, without step 10).

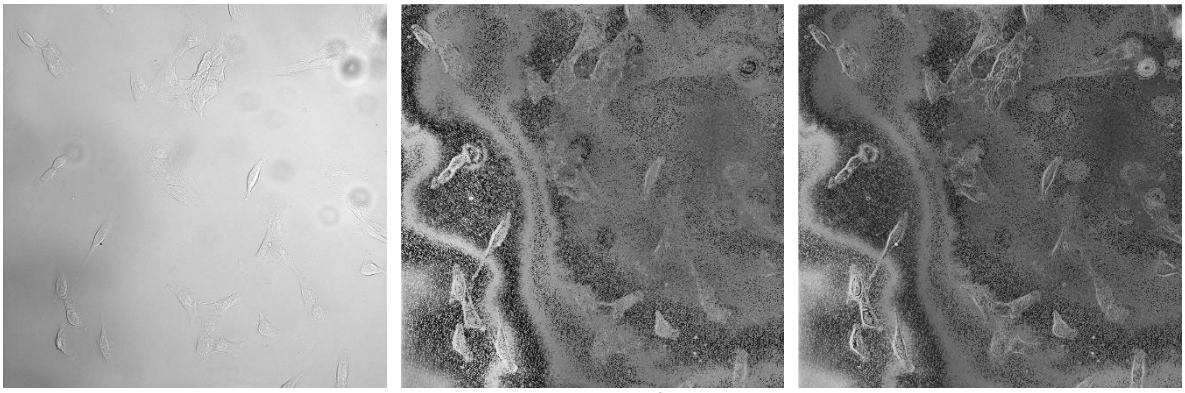

a b c

Figure 7: Segmentation results of a microbiological image: (a) original image (1024×1024); (b) orthogonal membership function space ($I^{out}$, without step 10); (c) complex orthogonal membership function space ($I^{out-c}$).

## 6. Conclusions

The effectiveness of fuzzy clustering methods significantly depends on the approach used to synthesize the final result based on membership functions. When designing an algorithm for

solving specific segmentation tasks, achieving practically significant results and validating their reliability may require the integration of multiple complementary methods.

The presented grayscale image segmentation algorithm, based on Type-2 fuzzy clustering, synthesizes a composite segmented image using multidimensional analysis methods. The core of this approach is built upon two key concepts: orthogonalization of membership functions and transition to the complex space of orthogonal membership functions. This approach enables the analysis of the entire set of membership functions as a unified whole while simultaneously interpreting the results as an anisotropic filtering process in a fuzzy space. This, in turn, enhances segmentation sensitivity and accuracy. While transitioning to the complex orthogonal membership function space results in a slight reduction in detail, it effectively minimizes the influence of noise components.

The proposed algorithm is effective for segmenting images of various physical natures, with the diagnostic significance of the extracted features being determined by the characteristics of the original data and the objectives of the analysis.

Promising directions for future research are the exploration of different orthogonalization methods for membership function ensembles, as well as investigating alternative functional dependencies for computing the coefficient $K_1$.

## Declaration on Generative AI

The authors have not employed any Generative AI tools.

## References


[1] R. Szeliski, Computer Vision: Algorithms and Applications, Cham: Springer, 2022. doi: 10.1007/978-3-030-34372-9.

[2] K. Cohen, N. Ernest, B. Bede, V. Kreinovich, Fuzzy Information Processing, Cham: Springer, 2023. doi: 10.1007/978-3-031-46778-3.

[3] A. Yegorov, L. Akhmetshina, Optimizaciya yarkosti izobrazhenij na osnove nejro-fazzi tehnologij. Monografiya. Lambert, Dnipro, 2015.

[4] W. Pedrycz, An Introduction to Computing with Fuzzy Sets, Vol. 190, Cham: Springer, 2020. doi: 10.1007/978-3-030-52800-3.

[5] I. Bloch, Fuzzy Sets for Image Processing and Understanding, Fuzzy Sets and Systems, 281 (2015) 280–291. doi: 10.1016/j.fss.2015.06.017.

[6] A. M. Ikhsan, A. Hussain, M. A. Zulkifley, N. Tahi, An analysis of X-ray image enhancement methods for vertebral bone segmentation, in: Signal Processing & its Applications (CSPA), Proceedings of 10th International Colloquium, IEEE, Kuala Lumpur, 2014, pp. 208–211. doi: 10.1109/CSPA.2014.6805749.

[7] J. Krayla, S. Kumar, U. K. Acharya, Analysis of Fuzzy Logic-based Image Enhancement Techniques for MRI Brain Images, in: R. Asokan, D. P. Ruiz, Z. A. Baig, S. Piramuthu (Eds.) Smart Data Intelligence. Algorithms for Intelligent Systems, Springer, Singapore, 2022, pp. 447–458. doi: 10.1007/978-981-19-3311-0_38.

[8] Y. Yu, Y. Wang, Q. Fu, G. Shi, Techniques and Challenges of Image Segmentation: A Review, Electronics. 12 5 (2023) Article 1199. doi: 10.3390/electronics12051199.

[9] L. A. Zadeh, Fuzzy sets and their application to pattern recognition and clustering analysis, in: Classification and Clustering, Proceedings of an Advanced Seminar Conducted by the Mathematics Research Center, the University of Wisconsin–Madison, Academic Press, New York, 1977, pp. 251–299. doi: 10.1016/B978-0-12-714250-0.50014-0.

[10] I. Bloch, A. Ralescu, Fuzzy Sets Methods in Image Processing and Understanding: Medical Imaging Applications, Cham: Springer, 2023. doi: 10.1007/978-3-031-19425-2.

[11] A. Nirmala, Medical Image Denoising by Nonlocal Means with Level Set Based Fuzzy Segmentation, Indian Journal of Science and Technology, 10 36 (2017) 1–11. doi: 10.17485/ijst/2017/v10i36/112402.

[12] T. Chaira, A novel intuitionistic fuzzy C-means clustering algorithm and its application to medical images, Applied Soft Computing, 11 2 (2011) 1711–1717. doi: 10.1016/j.asoc.2010.12.007.

[13] E. Pichon, A. Tannenbaum, S. Angenent, Mathematical methods in medical image processing, Bulletin (New Series) of the American Mathematical Society, 43 3 (2006) 365–396. doi: 10.1090/s0273-0979-06-01104-9.
[14] F. U. Siddiqui, A. Yahya, Clustering Techniques for Image Segmentation, Cham: Springer Nature Switzerland AG, 2021. doi: 10.1007/978-3-030-81230-0.
[15] W. Pedrycz, An Introduction to Computing with Fuzzy Sets: Analysis, Design, and Applications, Cham: Springer, 2021. doi: 10.1007/978-3-030-52800-3.
[16] L. Akhmetshina, A. Yegorov, Low-Contrast Image Segmentation by Using of the Type-2 Fuzzy Clustering Based on the Membership Function Statistical Characteristics, in: Intellectual Systems of Decision Making and Problems of Computational Intelligence (ISDMCI), Proceedings of XV International Scientific Conference, Springer, Kherson, 2019, pp. 689–700.
[17] J. M. Mendel, Uncertain Rule Based Fuzzy Systems, Cham: Springer, 2023. doi: 10.1007/978-3-031-35378-9.
[18] S. Begum, O. M. Devi, A Rough, Type-2 Fuzzy Clustering Algorithm for MR Image Segmentation, International Journal of Computer Applications, 54 4 (2012) 4–11. doi: 10.5120/8552-2114.
[19] S. Peng, C. Wu, Deep Neighborhood Structure Driven Interval Type 2 Kernel Fuzzy C Means Clustering, Multimedia Tools and Applications, 82 28 (2023) 43455–43515. doi: 10.1007/s11042-023-15230-2.
[20] C. Wang, W. Pedrycz, Z. Li, M. Zhou, Residual Driven Fuzzy C Means Clustering for Image Segmentation, IEEE/CAA Journal of Automatica Sinica, 8 4 (2021) 876–889. doi: 10.1109/JAS.2020.1003420.
[21] K. Pearson, On lines and planes of closest fit to systems of points in space, The London, Edinburgh, and Dublin Philosophical Magazine and Journal of Science, 2 11 (1901) 559–572. doi: 10.1080/14786440109462720.
[22] J. Yang, D. Zhang, A. F. Frangi, J.-Y Yang, Two-dimensional PCA: A new approach to appearance-based face representation and recognition, IEEE Transactions on Pattern Analysis and Machine Intelligence, 26 1 (2004) 131–137. doi: 10.1109/TPAMI.2004.1261097.
[23] L. G. Akhmetshina, A. A. Yegorov, Adaptivnaya nechetkaya segmentatsiya izobrazhenij na osnove kombinirovannogo singulyarnogo razlozheniya, Vestnik KNTU, 3(54) (2016) 198–202.
[24] H. Hoteling, Analysis of a complex of statistical variables into principal components, Journal of Educational Psychology, 24, № 6 (1933) 417–441. doi: 10.1037/h0071325.
[25] L. G. Akhmetshina, A. A. Yegorov, Segmentaciya slabokontrastnyh izobrazhenij v ortogonal'nom bazise funkcij prinadlezhnosti nechetkoj klasterizacii, Visnyk Hersons'kogo nacional'nogo tehnichnogo universytetu 2(69) 2 (2019) 160–165.